1 Supplementary material for LHCb-PAPER-2018-051

1.1 Further tables and plots for the nominal solution

The results of the nominal solution as function of $x, y, \Delta x, \Delta y$ is shown in Table 2. Its corresponding correlation matrix is presented in Table 3.

Table 2: Dalitz plot fit results of the nominal solution as function of $x, y, \Delta x, \Delta y$, where the uncertainty presented is statistical only.

Component	x	y	Δx	Δy
$K^*(892)^0$	1.00 (fixed)	0 (fixed)	-0.06 ± 0.04	0 (fixed)
$K_0^*(1430)^0$	-0.66 ± 0.08	0.26 ± 0.09	-0.07 ± 0.08	-0.31 ± 0.08
Single-Pole	-1.77 ± 0.16	-0.49 ± 0.15	0.14 ± 0.11	-0.97 ± 0.16
$\rho(1450)^0$	-1.80 ± 0.16	0.53 ± 0.24	-0.33 ± 0.14	-0.70 ± 0.25
$f_2(1270)$	-0.46 ± 0.13	-0.86 ± 0.09	0.23 ± 0.13	0.03 ± 0.09
rescattering	0.60 ± 0.19	-1.22 ± 0.13	0.46 ± 0.20	-0.37 ± 0.12
$\phi(1020)$	0.03 ± 0.07	0.03 ± 0.05	0.09 ± 0.07	-0.18 ± 0.05

Projections of the nominal solution, separated by charge, are shown in Figs. 4, 5 and 6. The Dalitz plot of the B^+ and B^- candidates is shown in Fig. 7.

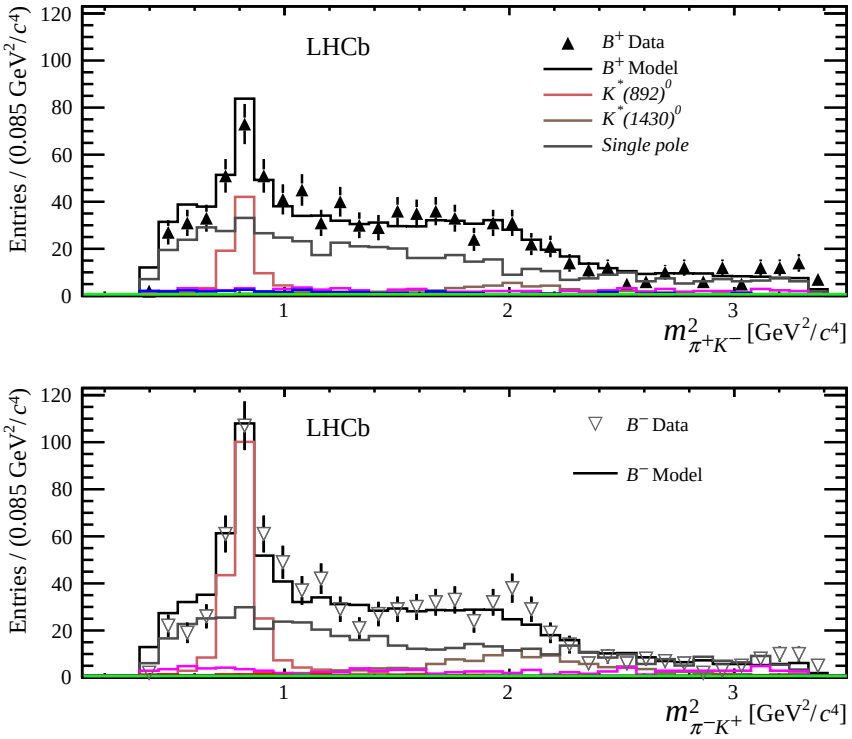

Figure 4: Distribution of $m^2_{\pi^\pm K^\mp}$ up to 3.5 GeV$^2/c^4$. Data are represented by points for B^+ and B^- candidates separately, with the result of the nominal solution overlaid. The relative contribution of the individual components in the model is also shown, with the interference terms effects not included.

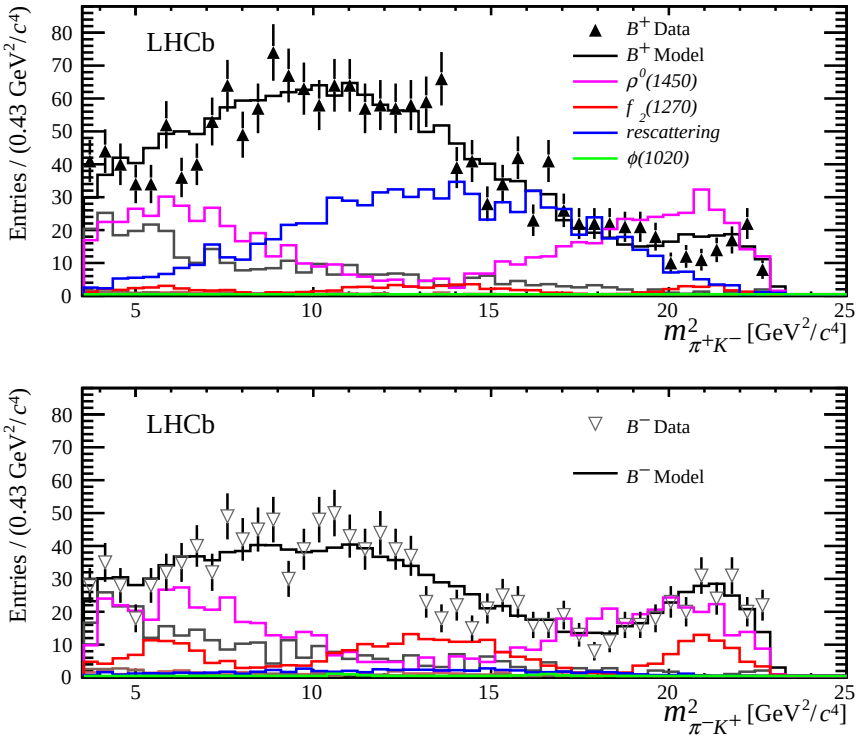

Figure 5: Distribution of $m^2_{\pi^\pm K^\mp}$ in the high mass region. Data are represented by points for (top) B^+ and (bottom) B^- with the result of the nominal solution overlaid. The relative contribution of the individual components in the model is also shown, with the interference terms effects not included.

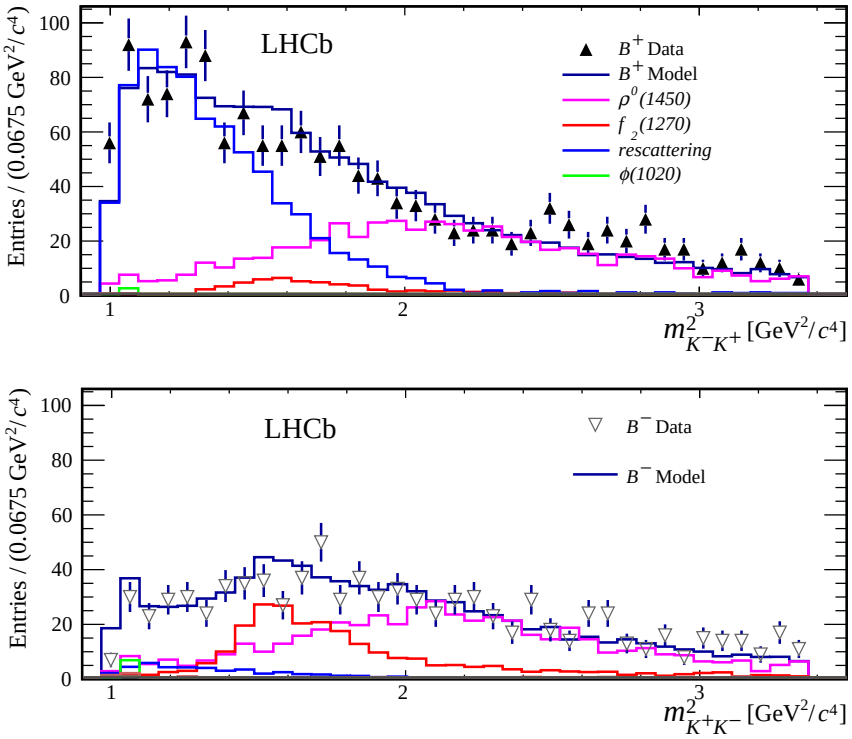

Figure 6: Distribution of $m^2_{K^+K^-}$ up to 3.5 GeV$^2/c^4$. Data are represented by points for B^+ and B^- candidates separately, with the result of the nominal solution overlaid. The relative contribution of the individual components in the model is also shown, with the interference terms effects not included.

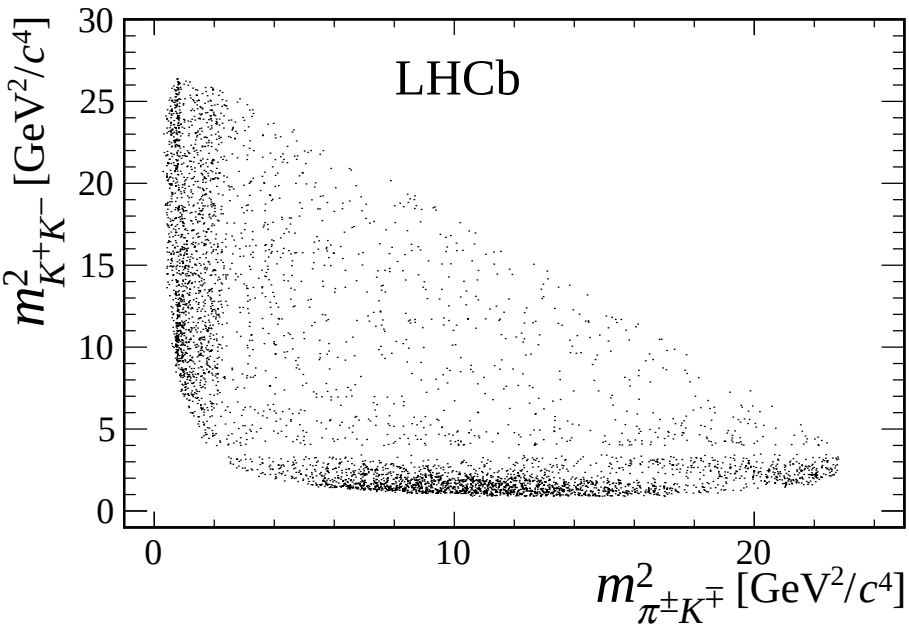

Figure 7: Dalitz plot for $B^+ \to \pi^+ K^- K^+$ and $B^- \to \pi^- K^+ K^-$ candidates in the selected signal region.

Table 3: Correlation matrix for the nominal solution.
$K^{*0}(892)$: par 3 = Δx. $K_0^*(1430)^0$: par 5,6,7,8 = $x, y, \Delta x, \Delta y$. NR Single-Pole Form Factor: par 9,10,11,12 = $x, y, \Delta x, \Delta y$. $\rho(1450)^0$: par 13,14,15,16 = $x, y, \Delta x, \Delta y$. $f_2(1270)$: par 17,18,19,20 = $x, y, \Delta x, \Delta y$. Rescattering: par 21,22,23,24 = $x, y, \Delta x, \Delta y$. $\phi(1020)$: par 24,26,27,28 = $x, y, \Delta x, \Delta y$.

	3	5	6	7	8	9	10	11	12.	13	14	15	16.	17	18	19.	20	21	22	23	24	25	26	27	28
3	1.0	0.068	-0.217	0.038	-0.113	0.339	-0.129	0.359	-0.216	0.180	-0.116	-0.023	-0.139	0.100	0.103	0.112	-0.088	0.064	0.195	0.120	0.163	0.054	0.036	-0.008	0.054
5		1.0	0.163	-0.407	-0.274	0.257	0.159	-0.030	-0.246	0.238	0.039	-0.024	0.041	0.020	0.244	0.000	-0.030	-0.118	0.107	-0.045	0.002	0.010	-0.010	-0.049	0.034
6			1.0	-0.275	0.188	-0.318	0.533	-0.591	0.089	-0.138	0.161	-0.044	0.094	-0.164	-0.054	-0.063	0.040	-0.098	-0.210	-0.098	-0.153	-0.031	-0.034	-0.018	-0.070
7				1.0	0.287	-0.067	-0.333	-0.013	0.207	-0.073	0.026	0.091	0.140	0.012	-0.020	-0.086	0.138	-0.044	-0.072	-0.124	-0.088	-0.051	-0.035	0.015	-0.005
8					1.0	-0.404	0.093	-0.194	0.521	-0.052	0.090	0.006	0.121	0.053	-0.006	-0.121	0.065	-0.090	-0.099	-0.114	-0.106	-0.033	-0.030	-0.021	-0.037
9						1.0	-0.293	0.572	-0.382	0.485	-0.347	0.016	-0.324	0.301	0.275	0.297	-0.203	0.190	0.577	0.306	0.456	0.113	0.092	0.011	0.184
10							1.0	-0.650	-0.164	0.313	0.618	-0.512	-0.043	-0.604	0.425	0.144	-0.337	-0.503	-0.365	-0.024	-0.238	0.087	-0.006	-0.229	-0.161
11								1.0	-0.320	0.060	-0.497	0.192	-0.284	0.437	-0.109	0.207	-0.033	0.420	0.469	0.306	0.401	0.055	0.088	0.136	0.165
12									1.0	-0.421	-0.052	0.459	0.634	0.164	-0.301	-0.612	0.519	-0.047	-0.163	-0.535	-0.350	-0.252	-0.153	0.090	0.007
13										1.0	0.339	-0.712	-0.589	-0.382	0.737	0.619	-0.695	-0.293	0.215	0.479	0.340	0.310	0.183	-0.269	-0.000
14											1.0	-0.646	0.155	-0.822	0.520	0.0238	-0.301	-0.794	-0.708	-0.218	-0.532	0.034	-0.080	-0.304	-0.266
15												1.0	0.559	0.680	-0.657	-0.604	0.689	0.488	0.244	-0.375	-0.048	-0.311	-0.109	0.331	0.213
16													1.0	0.0416	-0.322	-0.826	0.686	-0.235	-0.446	-0.834	-0.693	-0.335	-0.242	0.043	-0.078
17														1.0	-0.492	-0.171	0.449	0.729	0.589	0.069	0.408	-0.138	0.038	0.300	0.262
18															1.0	0.461	-0.524	-0.566	-0.132	0.204	-0.006	0.213	0.020	-0.276	-0.085
19																1.0	-0.659	0.095	0.350	0.777	0.566	0.328	0.237	-0.141	0.044
20																	1.0	0.179	-0.145	-0.632	-0.416	-0.305	-0.170	0.218	0.005
21																		1.0	0.732	0.396	0.673	-0.106	0.169	0.298	0.294
22																			1.0	0.609	0.833	0.094	0.235	0.116	0.305
23																				1.0	0.830	0.318	0.306	-0.117	0.161
24																					1.0	0.158	0.254	0.085	0.295
25																						1.0	0.275	-0.417	-0.217
26																							1.0	-0.225	0.115
27																								1.0	0.267
28																									1.0

1.2 Second fit solution

In the following the results and projections of the second solution are presented in Table 4 and Figs. 8, 9, 10. This is interpreted as an unphysical solution.

Table 4: Results of the Dalitz plot fit using the isobar model for the second solution, where the uncertainty presented is statistical only. This solution is interpreted as unphysical.

	Fit fraction (%)		Magnitude and phase coefficients				A_{CP} (%)
Component	B^+	B^-	a_i^+	$\delta_i^+[^\circ]$	a_i^-	$\delta_i^-[^\circ]$	
$K^*(892)^0$	5.7 ± 0.8	10.4 ± 1.0	0.93 ± 0.04	0 (fixed)	1.07 ± 0.04	0 (fixed)	14.9 ± 8.6
$K_0^*(1430)^0$	3.5 ± 1.2	34.9 ± 3.7	0.73 ± 0.15	-176 ± 10	1.97 ± 0.14	-149 ± 3	76.1 ± 10.2
Single-Pole	30.9 ± 1.9	31.0 ± 3.0	2.16 ± 0.13	-138 ± 7	1.86 ± 0.13	140 ± 7	-15.0 ± 5.9
$\rho(1450)^0$	29.5 ± 1.8	32.4 ± 2.1	2.11 ± 0.11	-175 ± 10	1.90 ± 0.10	77 ± 13	-10.6 ± 4.4
$f_2(1270)$	4.7 ± 0.9	10.8 ± 1.4	0.84 ± 0.09	-106 ± 11	1.10 ± 0.08	170 ± 5	25.7 ± 10.3
rescattering	23.7 ± 1.3	6.8 ± 0.9	1.89 ± 0.09	-57 ± 12	0.87 ± 0.07	-145 ± 17	-65.0 ± 3.9
$\phi(1020)$	0.2 ± 0.2	0.4 ± 0.2	0.19 ± 0.07	-53 ± 23	0.22 ± 0.06	42 ± 30	11.2 ± 43.1
Sum	98.3	126.7					

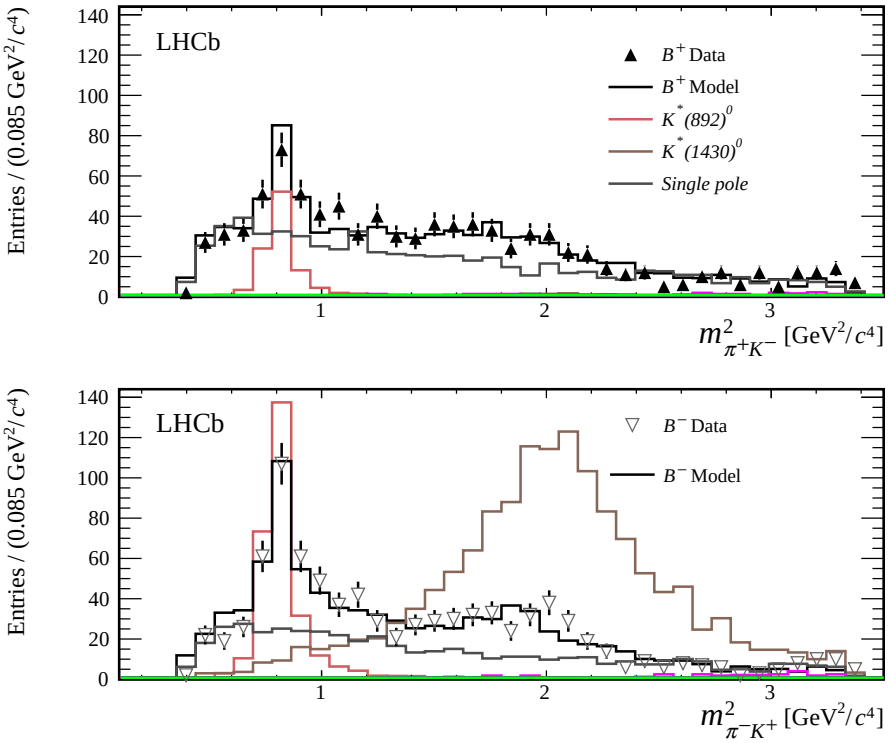

Figure 8: Distribution of $m^2_{\pi^\pm K^\mp}$ up to 3.5 GeV$^2/c^4$. Data are represented by points for B^+ and B^- candidates separately, with the result of the second solution overlaid. This is interpreted as an unphysical solution. The relative contribution of the individual components in the model is also shown, with the interference terms effects not included.

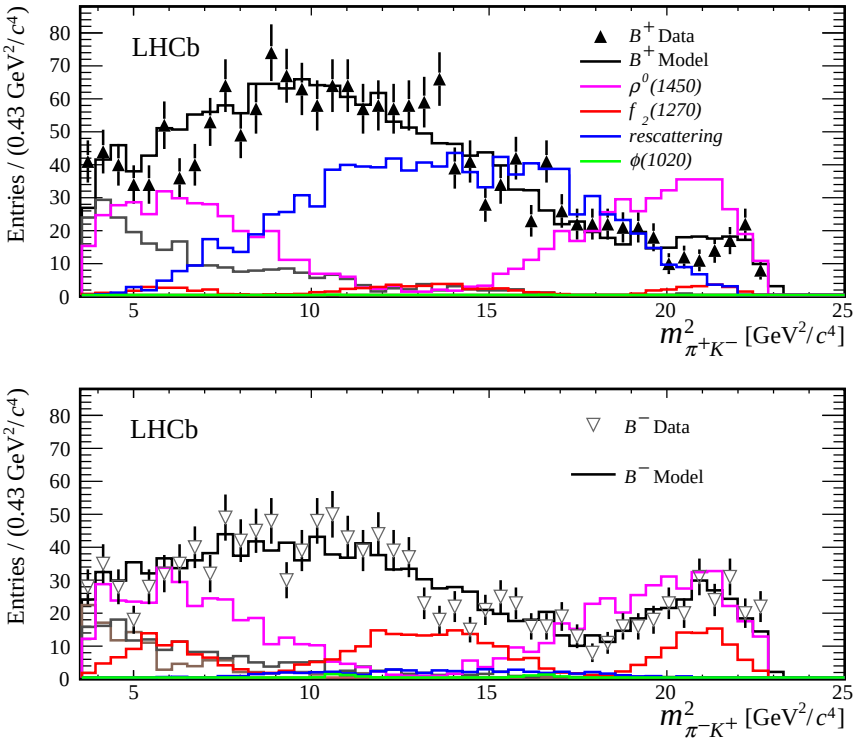

Figure 9: Distribution of $m^2_{\pi^\pm K^\mp}$ in the high mass region. Data are represented by points for (top) B^+ and (bottom) B^- with the result of the second solution overlaid. This is interpreted as an unphysical solution. The relative contribution of the individual components in the model is also shown, with the interference terms effects not included.

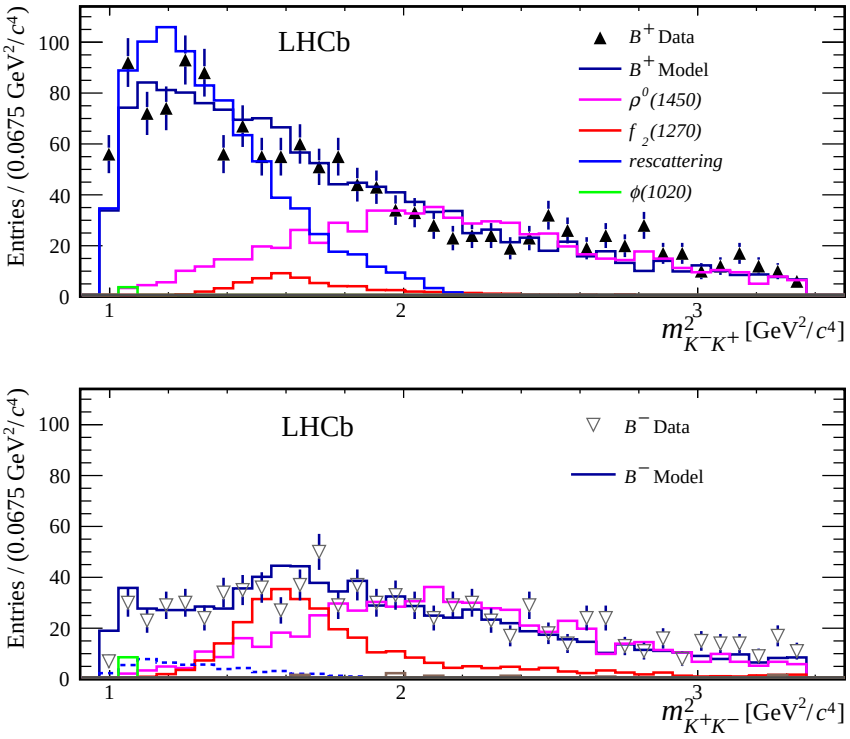

Figure 10: Distribution of $m^2_{K^+K^-}$ up to 3.5 GeV$^2/c^4$. Data are represented by points for B^+ and B^- candidates separately, with the result of the second solution overlaid. This is interpreted as an unphysical solution. The relative contribution of the individual components in the model is also shown, with the interference terms effects not included.

The results of the second solution given as function of $x, y, \Delta x, \Delta y$ is shown in Table 5. Its corresponding correlation matrix is presented in Table. 6.

Table 5: Dalitz plot fit results of the second solution as function of $x, y, \Delta x, \Delta y$, where the uncertainty presented is statistical only.

Component	x	y	Δx	Δy
$K^*(892)^0$	1.00 (fixed)	0 (fixed)	-0.08 ± 0.04	0 (fixed)
$K_0^*(1430)^0$	-1.21 ± 0.10	-0.53 ± 0.12	0.48 ± 0.08	0.48 ± 0.13
Single-Pole	-1.51 ± 0.16	-0.12 ± 0.13	-0.09 ± 0.13	-1.32 ± 0.13
$\rho(1450)^0$	-0.83 ± 0.21	0.84 ± 0.20	-1.27 ± 0.23	-1.01 ± 0.19
$f_2(1270)$	-0.66 ± 0.10	-0.31 ± 0.13	0.42 ± 0.09	-0.50 ± 0.13
rescattering	0.16 ± 0.18	-1.04 ± 0.15	0.88 ± 0.18	-0.54 ± 0.15
$\phi(1020)$	0.14 ± 0.06	-0.01 ± 0.06	-0.02 ± 0.06	-0.15 ± 0.06

Table 6: Correlation matrix for the second solution. This is interpreted as an unphysical solution. $K^*(892)^0$: par 3 = Δx. $K_0^*(1430)^0$: par 5,6,7,8 = $x, y, \Delta x, \Delta y$. NR Single-Pole Form Factor: par 9,10,11,12 = $x, y, \Delta x, \Delta y$. $\rho(1450)^0$: par 13,14,15,16 = $x, y, \Delta x, \Delta y$. $f_2(1270)$: par 17,18,19,20 = $x, y, \Delta x, \Delta y$. Rescattering: par 21,22,23,24 = $x, y, \Delta x, \Delta y$. $\phi(1020)$: par 24,26,27,28 = $x, y, \Delta x, \Delta y$.

	3	5	6	7	8	9	10	11	12.	13	14	15	16.	17	18	19.	20	21	22	23	24	25	26	27	28
3	1.0	0.057	0.005	-0.035	-0.216	0.338	-0.172	0.268	-0.217	0.123	-0.212	-0.010	-0.090	0.212	0.062	0.065	-0.050	0.094	0.197	0.106	0.092	0.036	0.002	0.016	0.074
5		1.0	-0.437	0.515	0.326	0.073	-0.546	0.441	0.475	-0.214	-0.023	0.464	0.060	0.137	-0.227	-0.034	0.424	0.073	0.008	-0.250	0.257	-0.157	0.108	0.108	-0.043
6			1.0	-0.537	-0.464	0.205	0.615	-0.602	-0.164	0.333	-0.016	-0.325	0.160	-0.003	0.361	-0.130	-0.324	-0.181	0.133	0.051	-0.221	0.076	-0.124	-0.112	0.094
7				1.0	0.469	-0.069	-0.427	0.523	0.574	-0.295	-0.109	0.428	-0.165	0.114	-0.353	0.097	0.354	0.226	0.013	-0.070	0.339	-0.111	0.146	0.140	-0.059
8					1.0	-0.631	-0.090	0.144	0.575	-0.367	0.227	0.258	-0.008	-0.208	-0.334	-0.007	0.318	0.019	-0.292	-0.172	0.074	-0.100	0.083	0.061	-0.147
9						1.0	-0.306	0.286	-0.436	0.463	-0.580	-0.138	-0.186	0.584	0.316	0.167	-0.276	0.208	0.602	0.331	0.182	0.128	-0.021	0.016	0.24
10							1.0	-0.799	0.102	0.167	0.423	-0.333	0.462	-0.401	0.289	-0.409	-0.221	-0.452	-0.234	-0.241	-0.474	-0.016	-0.159	-0.181	-0.036
11								1.0	-0.104	-0.364	-0.352	0.532	-0.476	0.352	-0.464	0.428	0.397	0.513	0.133	0.145	0.559	-0.052	0.221	0.233	-0.021
12									1.0	-0.258	0.383	0.301	0.372	-0.297	-0.184	-0.331	0.365	-0.242	-0.309	-0.467	-0.055	-0.195	0.017	-0.013	-0.126
13										1.0	-0.330	-0.863	0.204	0.287	0.832	-0.174	-0.823	-0.256	0.560	0.392	-0.407	0.254	-0.229	-0.221	0.300
14											1.0	0.101	0.754	-0.773	-0.095	-0.602	0.295	-0.638	-0.781	-0.739	-0.530	-0.264	-0.085	-0.124	-0.283
15												1.0	-0.264	-0.036	-0.812	0.224	0.840	0.405	-0.301	-0.306	0.597	-0.250	0.292	0.269	-0.190
16													1.0	-0.580	0.368	-0.744	-0.067	-0.804	-0.447	-0.642	-0.704	-0.117	-0.257	-0.295	-0.073
17														1.0	0.573	0.098	-0.158	0.561	0.653	0.720	0.484	0.144	0.122	0.110	0.254
18															1.0	-0.251	-0.776	-0.462	0.346	0.166	-0.610	0.205	-0.306	-0.260	0.226
19																1.0	0.074	0.750	0.385	0.568	0.630	0.110	0.226	0.184	0.095
20																	1.0	0.175	-0.524	-0.488	0.394	-0.278	0.231	0.214	-0.280
21																		1.0	0.476	0.655	0.898	0.031	0.339	0.219	0.109
22																			1.0	0.812	0.288	0.260	-0.026	-0.039	0.415
23																				1.0	0.408	0.226	0.087	0.028	0.323
24																					1.0	-0.090	0.403	0.313	-0.015
25																						1.0	-0.354	-0.243	0.389
26																							1.0	0.402	-0.199
27																								1.0	-0.341
28																									1.0

1.3 Systematic uncertainties

The systematic uncertainties for *CP* asymmetries, total fit fractions, B^+ and B^- fit fractions, magnitudes and phases for the $B^\pm \to \pi^\pm K^+ K^-$ Dalitz plot fit are shown in Tables 7 to 11, respectively.

Table 7: Systematic uncertainties for the *CP* asymmetries (in percent).

A_{CP}	$K^*(892)$	$K_0^*(1430)^0$	Single pole	$\rho(1450)^0$	$f_2(1270)$	Rescattering	$\phi(1020)$
Statistical uncertainty	**8.7**	**14.9**	**5.3**	**4.4**	**10.2**	**3.8**	**43.6**
$B^\pm$ mass fit							
Maximum value	2.6	2.63	2.01	0.28	0.08	0.26	10.11
Minimum value	0.26	0.35	0.3	0.25	0.73	0.14	14.27
Efficiency model							
Simulation sample size	0.54	0.9	0.27	0.37	0.83	0.39	2.47
PID	1.75	0.41	0.12	0.03	0.07	0.01	0.06
L0 trigger correction	0.55	0.18	0.16	0.01	0.21	0.02	0.03
Finer binning	0.96	0.11	0.15	0.02	1.01	0.23	0.2
Coarse binning	0.19	1.4	0.21	0.17	2.05	0.07	2.21
B^+ production and detection asymmetry	1.49	1.51	1.48	1.48	1.39	0.85	1.47
MC truth requirement	0.03	0.01	0.0	0.0	0.02	0.0	0.01
Background models							
Combinatorial background	1.34	1.19	0.42	0.19	0.85	0.37	2.52
Peaking background	0.19	0.24	0.08	0.09	0.15	0.09	0.89
Isobar Model							
Fit bias	0.63	0.94	0.22	0.16	0.84	0.19	0.23
Blatt Weisskopf radii set in 3 GeV^{-1}	0.9	1.39	0.83	0.36	2.79	1.04	2.78
Blatt Weisskopf radii set in 5 GeV^{-1}	0.41	0.39	0.43	0.33	1.24	0.8	3.39
Mass and width variation	0.82	7.52	1.6	0.34	1.07	0.65	7.52
ϕ background level							
Upward	0.1	0.06	0.06	0.07	0.42	0.07	9.14
Downward	0.12	0.12	0.1	0.12	0.42	0.11	9.66
$\rho(1450)$ free to float in the fit	1.67	1.97	1.33	1.63	1.58	0.64	11.34
Total systematic uncertainty	**4.51**	**8.78**	**3.45**	**2.36**	**4.81**	**1.94**	**26.59**

Table 8: Systematic uncertainties for the total fit fractions (in percent).

Total fit fraction FF	$K^*(892)$	$K_0^*(1430)^0$	Single pole	$\rho(1450)^0$	$f_2(1270)$	Rescattering	$\phi(1020)$
Statistical uncertainty	**0.60**	**0.68**	**1.54**	**1.22**	**0.82**	**0.75**	**0.13**
$B^\pm$ mass fit							
Maximum value	0.38	0.78	2.0	0.25	0.06	0.55	0.01
Minimum value	0.04	0.19	0.51	0.08	0.07	0.44	0.05
Efficiency model							
Statistical fluctuation	0.04	0.04	0.09	0.09	0.07	0.09	0.01
PID	0.1	0.02	0.04	0.04	0.01	0.02	0.0
L0 trigger correction	0.03	0.01	0.05	0.03	0.01	0.04	0.0
Finer binning	0.01	0.02	0.05	0.11	0.05	0.13	0.01
Coarse binning	0.03	0.01	0.09	0.09	0.01	0.05	0.0
B production and detection asymmetry	0.03	0.02	0.02	0.02	0.05	0.13	0.0
MC truth requirement	0.0	0.0	0.0	0.0	0.0	0.0	0.0
Background models							
Combinatorial background	0.11	0.23	0.48	0.31	0.17	0.17	0.0
Peaking background	0.02	0.03	0.1	0.11	0.04	0.05	0.0
Isobar model							
Fit bias	0.22	0.05	0.19	0.04	0.0	0.02	0.05
Blatt Weisskopf radii set in 3 GeV^{-1}	0.03	0.38	0.13	0.02	0.12	0.29	0.01
Blatt Weisskopf radii set in 5 GeV^{-1}	0.01	0.21	0.14	0.1	0.04	0.21	0.0
Mass and Width variation	0.19	0.76	3.45	0.79	0.23	0.35	0.01
ϕ background level							
Upward	0.01	0.06	0.23	0.08	0.05	0.24	0.03
Downward	0.01	0.06	0.25	0.09	0.05	0.27	0.03
$\rho(1450)$ free to float in the fit	0.07	0.22	0.17	0.03	0.6	0.0	0.03
Total systematic uncertainty	**0.51**	**1.23**	**4.07**	**0.92**	**0.69**	**0.97**	**0.09**

Table 9: Systematic uncertainties for B^+ and B^- fit fractions (in percent).

B^+ **Fit fraction: FF$^+$**	$K^*(892)$	$K_0^*(1430)^0$	Single pole	$\rho(1450)^0$	$f_2(1270)$	Rescattering	$\phi(1020)$
Statistical uncertainty	**0.8**	**0.8**	**2.0**	**1.5**	**0.9**	**1.1**	**0.2**
$B^\pm$ mass fit							
Maximum value	0.1	0.5	1.52	0.02	0.0	0.68	0.02
Minimum value	0.0	0.13	0.46	0.19	0.1	0.57	0.01
Efficiency model							
Simulation sample size	0.05	0.05	0.13	0.12	0.08	0.14	0.01
PID	0.18	0.03	0.07	0.06	0.02	0.06	0.0
L0 trigger correction	0.06	0.0	0.07	0.05	0.01	0.08	0.0
Finer binning	0.05	0.01	0.01	0.09	0.03	0.17	0.01
Coarse binning	0.02	0.06	0.0	0.15	0.14	0.04	0.01
B production and detection asymmetry	0.0	0.0	0.0	0.0	0.0	0.0	0.0
MC truth requirement	0.0	0.0	0.0	0.0	0.0	0.0	0.0
Background models							
Combinatorial background	0.16	0.17	0.43	0.31	0.16	0.19	0.01
Peaking background	0.02	0.02	0.08	0.1	0.03	0.06	0.0
Isobar Model							
Fit bias	0.13	0.07	0.13	0.01	0.06	0.07	0.05
Blatt Weisskopf radii set in 3 GeV^{-1}	0.03	0.24	0.13	0.14	0.25	0.29	0.02
Blatt Weisskopf radii set in 5 GeV^{-1}	0.02	0.15	0.0	0.0	0.05	0.2	0.01
Mass and width variation	0.11	0.8	3.0	0.79	0.22	0.42	0.02
ϕ background level							
Upward	0.0	0.04	0.22	0.12	0.06	0.32	0.0
Downward	0.01	0.04	0.24	0.14	0.07	0.35	0.0
$\rho(1450)$ free to float in the fit	0.16	0.09	0.56	0.38	0.49	0.11	0.06
Total systematic uncertainty	**0.36**	**1.01**	**3.49**	**1.00**	**0.65**	**1.19**	**0.08**

B^- **Fit fraction: FF$^-$**	$K^*(892)$	$K_0^*(1430)^0$	Single pole	$\rho(1450)^0$	$f_2(1270)$	Rescattering	$\phi(1020)$
Statistical uncertainty	**1.0**	**1.2**	**2.6**	**1.9**	**1.3**	**0.8**	**0.2**
$B^\pm$ mass fit							
Maximum value	0.8	1.17	2.61	0.63	0.19	0.22	0.04
Minimum value	0.1	0.28	0.57	0.09	0.01	0.22	0.13
Efficiency model							
Simulation sample size	0.07	0.05	0.13	0.13	0.1	0.07	0.01
PID	0.01	0.01	0.02	0.01	0.0	0.0	0.0
L0 trigger correction	0.01	0.01	0.02	0.0	0.02	0.01	0.0
Finer binning	0.09	0.03	0.13	0.15	0.15	0.09	0.02
Coarse binning	0.04	0.05	0.22	0.01	0.14	0.04	0.01
B production and detection asymmetry	0.0	0.0	0.0	0.0	0.0	0.0	0.0
MC truth requirement	0.0	0.0	0.0	0.0	0.0	0.0	0.0
Background models							
Combinatorial background	0.1	0.32	0.59	0.34	0.2	0.14	0.01
Peaking background	0.02	0.05	0.12	0.12	0.05	0.04	0.0
Isobar Model							
Fit bias	0.34	0.02	0.27	0.11	0.09	0.04	0.05
Blatt Weisskopf radii set in 3 GeV^{-1}	0.11	0.57	0.49	0.15	0.05	0.31	0.0
Blatt Weisskopf radii set in 5 GeV^{-1}	0.04	0.28	0.35	0.26	0.16	0.23	0.01
Mass and width variation	0.31	0.77	4.1	0.8	0.26	0.26	0.03
ϕ background level							
Upward	0.03	0.09	0.24	0.03	0.02	0.11	0.07
Downward	0.03	0.1	0.26	0.01	0.03	0.14	0.09
$\rho(1450)$ free to float in the fit	0.04	0.39	0.37	0.59	0.74	0.13	0.0
Total systematic uncertainty	**0.95**	**1.65**	**5.00**	**1.29**	**0.88**	**0.63**	**0.18**

Table 10: Systematic uncertainties for B^+ and B^- magnitudes.

B^+ magnitude: a^+	Resonant Components						
	$K^*(892)$	$K_0^*(1430)^0$	Single pole	$\rho(1450)^0$	$f_2(1270)$	Rescattering	$\phi(1020)$
Statistical uncertainty	**0.04**	**0.09**	**0.13**	**0.11**	**0.09**	**0.09**	**0.07**
$B^\pm$ mass fit							
Maximum value	0.01	0.04	0.1	0.05	0.02	0.01	0.0
Minimum value	0.0	0.01	0.02	0.01	0.01	0.02	0.0
Efficiency model							
Simulation sample size	0.0	0.01	0.01	0.01	0.01	0.01	0.0
PID	0.01	0.01	0.02	0.02	0.01	0.02	0.0
L0 trigger correction	0.0	0.0	0.0	0.01	0.0	0.01	0.0
Finer binning	0.0	0.0	0.0	0.0	0.0	0.01	0.0
Coarse binning	0.0	0.01	0.01	0.0	0.01	0.01	0.0
B production and detection asymmetry	0.01	0.01	0.02	0.02	0.01	0.02	0.0
MC truth requirement	0.0	0.0	0.0	0.0	0.0	0.0	0.0
Background models							
Combinatorial background	0.01	0.02	0.03	0.02	0.02	0.02	0.0
Peaking background	0.0	0.0	0.01	0.01	0.0	0.0	0.0
Isobar Model							
Fit bias	0.0	0.01	0.03	0.02	0.01	0.02	0.01
Blatt Weisskopf radii set in 3 GeV^{-1}	0.0	0.02	0.0	0.0	0.02	0.01	0.01
Blatt Weisskopf radii set in 5 GeV^{-1}	0.0	0.02	0.0	0.0	0.01	0.01	0.0
Mass and width variation	0.0	0.08	0.13	0.04	0.02	0.03	0.01
ϕ background level							
Upward	0.0	0.0	0.01	0.0	0.01	0.01	0.0
Downward	0.0	0.0	0.01	0.01	0.01	0.01	0.0
$\rho(1450)$ free to float in the fit	0.01	0.01	0.03	0.0	0.05	0.01	0.02
Total systematic uncertainty	**0.02**	**0.09**	**0.17**	**0.07**	**0.07**	**0.06**	**0.02**

B^- magnitude: a^-	$K^*(892)$	$K_0^*(1430)^0$	Single pole	$\rho(1450)^0$	$f_2(1270)$	Rescattering	$\phi(1020)$
Statistical uncertainty	**0.04**	**0.09**	**0.12**	**0.10**	**0.08**	**0.07**	**0.06**
$B^\pm$ mass fit							
Maximum value	0.01	0.06	0.14	0.04	0.02	0.01	0.02
Minimum value	0.0	0.02	0.02	0.0	0.0	0.01	0.03
Efficiency model							
Simulation sample size	0.0	0.0	0.01	0.01	0.01	0.01	0.0
PID	0.01	0.01	0.02	0.02	0.01	0.01	0.0
L0 trigger correction	0.0	0.0	0.01	0.01	0.0	0.0	0.0
Finer binning	0.0	0.0	0.0	0.0	0.01	0.01	0.0
Coarse binning	0.0	0.0	0.01	0.0	0.01	0.0	0.0
B production and detection asymmetry	0.01	0.01	0.01	0.01	0.01	0.01	0.0
MC truth requirement	0.0	0.0	0.0	0.0	0.0	0.0	0.0
Background models							
Combinatorial background	0.01	0.02	0.02	0.02	0.01	0.01	0.0
Peaking background	0.0	0.0	0.01	0.0	0.0	0.0	0.0
Isobar Model							
Fit bias	0.0	0.01	0.03	0.02	0.02	0.01	0.0
Blatt Weisskopf radii set in 3 GeV^{-1}	0.0	0.04	0.02	0.01	0.0	0.02	0.0
Blatt Weisskopf radii set in 5 GeV^{-1}	0.0	0.02	0.01	0.01	0.01	0.02	0.0
Mass and width variation	0.0	0.06	0.14	0.03	0.02	0.02	0.01
ϕ background level							
Upward	0.0	0.01	0.01	0.0	0.0	0.01	0.02
Downward	0.0	0.01	0.01	0.0	0.0	0.01	0.02
$\rho(1450)$ free to float in the fit	0.01	0.03	0.0	0.03	0.04	0.0	0.0
Total systematic uncertainty	**0.02**	**0.10**	**0.20**	**0.07**	**0.05**	**0.04**	**0.04**

Table 11: Systematic uncertainties for B^- and B^- phases (in degrees).

B^+ phase: δ^+	Component						
	$K^*(892)$	$K_0^*(1430)^0$	Single pole	$\rho(1450)^0$	$f_2(1270)$	Rescattering	$\phi(1020)$
Statistical uncertainty	**0** [fixed]	**10**	**7**	**10**	**11**	**12**	**23**
$B^\pm$ mass fit							
Maximum value	–	1.13	2.6	1.48	0.18	0.98	3.56
Minimum value	–	0.47	0.07	1.04	1.65	2.07	1.56
Efficiency model							
Simulation sample size	–	0.72	0.55	0.7	0.92	1.06	1.75
PID	–	1.58	1.38	1.12	1.12	1.1	1.07
L0 trigger correction	–	0.66	0.58	0.49	0.42	0.43	0.58
Finer binning	–	0.39	0.4	0.9	1.17	1.74	1.3
Coarse binning	–	0.38	0.74	0.27	0.35	0.24	0.36
B production and detection asymmetry	–	0.01	0.0	0.01	0.02	0.01	0.02
MC truth requirement	–	0.04	0.04	0.04	0.04	0.05	0.08
Background models							
Combinatorial background	–	2.57	1.66	3.03	3.09	3.04	3.16
Peaking background	–	0.52	0.32	0.41	0.48	0.53	0.55
Isobar model							
Fit bias	–	0.07	0.3	0.06	0.34	0.06	0.08
Blatt Weisskopf radii set in 3 GeV^{-1}	–	0.95	1.35	0.28	6.01	0.97	4.81
Blatt Weisskopf radii set in 5 GeV^{-1}	–	0.41	0.62	0.17	3.32	0.3	3.48
Mass and width variation	–	14.37	2.7	6.78	4.92	6.94	10.55
ϕ background level							
Upward	–	0.13	0.0	0.22	0.55	0.75	0.37
Downward	–	0.12	0.01	0.28	0.66	0.92	0.55
$\rho(1450)$ free to float in the fit	–	4.72	1.91	12.39	1.41	15.87	29.02
Total systematic uncertainty	–	**15.55**	**5.10**	**14.66**	**9.51**	**17.96**	**31.95**

B^- phase: δ^-	$K^*(892)$	$K_0^*(1430)^0$	Single pole	$\rho(1450)^0$	$f_2(1270)$	Rescattering	$\phi(1020)$
Statistical uncertainty	**0** [fixed]	**11**	**6**	**13**	**11**	**14**	**33**
$B^\pm$ mass fit							
Maximum value	–	2.15	0.85	2.94	3.36	3.85	2.25
Minimum value	–	1.0	0.48	2.52	2.75	3.51	4.94
Efficiency model							
Simulation sample size	–	0.61	0.41	0.71	0.74	0.88	1.16
PID	–	0.13	0.09	0.11	0.1	0.11	0.12
L0 trigger correction	–	0.48	0.42	0.2	0.15	0.15	0.19
Finer binning	–	0.06	0.34	0.44	0.77	0.33	2.07
Coarse binning	–	0.54	0.59	0.17	0.24	0.31	0.99
B production and detection asymmetry	–	0.0	0.0	0.02	0.02	0.02	0.04
MC truth requirement	–	0.03	0.02	0.01	0.01	0.01	0.02
Background models							
Combinatorial background	–	2.26	1.48	4.46	3.96	4.35	5.56
Peaking background	–	0.55	0.27	0.64	0.62	0.67	0.85
Isobar Model							
Fit bias	–	0.8	0.02	0.89	0.07	1.42	0.11
Blatt Weisskopf radii set in 3 GeV^{-1}	–	0.83	0.94	3.16	8.64	4.99	6.69
Blatt Weisskopf radii set in 5 GeV^{-1}	–	0.5	0.49	1.07	4.57	2.11	4.8
Mass and width variation	–	20.99	3.62	9.81	8.37	9.26	11.87
ϕ background level							
Upward	–	0.31	0.11	0.66	0.85	1.27	1.34
Downward	–	0.3	0.1	0.75	0.95	1.4	2.15
$\rho(1450)$ free to float in the fit	–	0.49	1.69	15.9	0.78	7.47	37.67
Total systematic uncertainty	–	**21.31**	**4.59**	**19.95**	**14.28**	**14.96**	**41.28**